



MODELING OF HUMAN KNEE JOINT IN SAGITTAL PLANE CONSIDERING ELASTIC BEHAVIOR OF CRUCIATE LIGAMENTS

Daniel Alejandro Ponce Saldias

Daniel Martins

Laboratório de Robótica, Universidade Federal de Santa Catarina, Campus Universitário, Trindade, Florianópolis/SC, Brasil.
danielpo25@gmail.com, daniel@emc.ufsc.br

Carlos Rodrigo de Mello Roesler, Fabíola da Silva Rosa, Ari Digiácomo Ocampo Moré

Laboratório de Engenharia Biomecânica, Universidade Federal de Santa Catarina, Hospital Universitário, Campus Universitário, Trindade, Florianópolis/SC, Brasil.

roesler@hu.ufsc.br, fahbysr@gmail.com, arimore@terra.com.br

Abstract. *The rupture of the anterior cruciate ligament (ACL) is the most common injury of the human knee and causes great instability to it, decreased functional ability as well as degeneration of the menisci and adjacent articular cartilage. When surgery is required, the preoperative planning becomes a critical step in defining the parameters to be used in surgery. In this context, orthopedic surgeons need to scientifically define the best insertion position of the graft, that approximates the functionality of an intact ACL, and also to know the pretension that the graft should be fixed. In addition to the factors listed above, it is interesting to estimate the force acting on the ligament (or graft) in response to an applied load on the knee. This force is called In-Situ force. The objective of the present research is to propose and to implement a methodology for computational modeling of the knee in the sagittal plane, considering elastic behavior of the ligaments, based on the theory of mechanisms and Davies method. The model should simulate the positions and In-Situ forces of a healthy ACL and also the pretension of the graft. This methodology will be used to implement custom models of the knee, to provide information to assist the medical decision making in the preoperative planning. The proposed methodology provides a unique and systematic approach for the biomechanical analysis of the knee, and it consists of four steps: Schematic representation of the physical model of the knee, Identification of the successive positions of the cruciate ligaments, Determining the cruciate ligaments forces, and Consideration of elastic behavior. The proposed methodology contemplates an experimental procedure performed to obtain the In-Situ forces. Experimental In-Situ forces serve to validate the proposed model. The experimental procedure is performed by a robotic manipulator that applies anterior tibial loads on a knee specimen, in several flexion angles. The robotic manipulator is coupled with an universal force sensor (UFS), that measures the In-Situ forces in the ACL. It can be concluded that the numeric results of the In-Situ forces and displacements that consider elastic behavior, are very close to the ones obtained in simulations which do not include elastic behavior of the ligaments. The simulated results are different from the experimental ones, because the proposed model is simplified and does not include tridimensional behaviors, such as axial knee rotation. It is possible to improve the results by adding a tridimensional model and the anatomical structures which were not considered in the proposed methodology, allowing the achievement of better simulation results, closer to the ones experimentally obtained.*

Keywords: *Computational modeling of the knee, preoperative planning, mechanisms, Davies method, elastic behavior.*

1. INTRODUCTION

The human knee joint is subjected to high mechanical solicitations when performing its biomechanical function and injuries are frequent. The rupture of the anterior cruciate ligament (ACL) is the most common injury on human knee (Woo *et al.*, 2006b) and causes great instability to it, decreased functional ability as well as degeneration of the menisci and adjacent articular cartilage. Cartilage problems and ligament injuries are treated surgically using grafts as a replacement of the ligaments, in case of ligament reconstruction, or using prosthesis, in case of osteoarthritis.

The surgical treatment for injuries involves the knee joint surgery, physiotherapy and rehabilitation procedures to restore the patient's functional abilities of the knee. For the surgery, the orthopedic surgeon must plan the surgery in order to obtain better results postoperatively. Therefore the preoperative planning is a critical step in selecting the surgical technique and the parameters definition to be used in surgery for each patient and, thus, it can directly affect the results of surgery.

For an appropriate preoperative planning, the orthopedic surgeon needs to know the exact problem to be solved (Sancisi and Parenti-Castelli, 2010; Olanlokun and Wills, 2002), possible surgical solutions (Sancisi and Parenti-Castelli, 2010; Olanlokun and Wills, 2002), the expected consequences for each solution (Olanlokun and Wills, 2002) and the physiotherapy protocol in the postoperative period (Sancisi and Parenti-Castelli, 2011b). In this context, several studies have been developed to define mechanical models representative of the knee. It has been shown that these models provide additional information to orthopedic doctors in several aspects of preoperative planning, as well as in the reconstruction

of ligaments, joint surfaces and osteotomy (Olanlokun and Wills, 2002). Moreover, these mechanical models are essential for the design of prostheses (Sancisi and Parenti-Castelli, 2010; Ottoboni *et al.*, 2005; Sancisi *et al.*, 2011), synthesis orthoses (Sancisi and Parenti-Castelli, 2010), and to estimate indirectly unmeasured forces that are internal to the joint (Sancisi *et al.*, 2011).

However, there still exist needs on the part of the orthopedic surgeons, such as: to obtain the scientific setting of the point for insertion of the graft that approximates the functionality of an intact ACL; to know the pretension that the graft should be fixed; and to estimate the force acting on the ligament (or graft) in response to an applied load to the knee. That force is called *In-Situ* force (Woo *et al.*, 2006a, 1998).

The main purposes of this work is to support the orthopedic surgeon to know the above mentioned requirements, using the information provided by a two-dimensional mechanical model of the knee, to be developed based on the mechanisms theory, the screw representation and the Davies method. This model allows to simulate the positions and forces of a healthy ACL in the sagittal plane, considering the elastic behavior of the cruciate ligaments. The model also allows to simulate the forces that occur in an ACL graft replacement, depending on the site of the graft insertion.

This being a multidisciplinary work, it begins with the biological theoretical foundations, which briefly covers the biomechanics of the knee in the sagittal plane. In the following section the theoretical backgrounds in robotics is presented, using it for analysis and modeling of the knee. The next section presents the proposed methodology for modeling, which consists of four sequential steps. In order to validate the proposed model, comparison were made between the simulated values of the *In Situ* force in the ACL with the experimetal ones, obtained by Woo *et al.* (1998). Finally, the conclusions are presented.

2. THEORICAL FOUNDATIONS IN KNEE BIOMECHANICS: FUNCTION OF THE CRUCIATE LIGAMENTS IN THE SAGITTAL PLANE

The function of the knee joint is the result of the interaction between the different parts that compose it. The interdependence of these structures are such that the injury of any of them leads to the deterioration of the joint as a whole (Woo *et al.*, 1998). Ligaments are particularly vulnerable because they are subject to sprains in almost all knee injuries, especially ACL. For this reason, the present study focused on the biomechanics of the cruciate ligaments and, specifically, on the ACL.

For a preliminary two-dimensional analysis of the knee, it is considered that the cruciate ligaments are behaving as inextensible cords or isometric links attached to bones (femur and tibia) through rotary joints. This consideration (Kapandji *et al.*, 2000; Wilson and O'Connor, 1997; Wilson *et al.*, 1998; Huson *et al.*, 1989; Gregorio and Parenti-Castelli, 2006; Parenti-Castelli *et al.*, 2004; Sancisi and Parenti-Castelli, 2011a, 2010, 2011b; Sancisi *et al.*, 2011), has the advantage of clarifying the general mechanical action of a ligament, but it does not allow to know the behavior in detail, because it does not take into account neither the viscoelastic effects, nor the other adjacent anatomical structures.

The geometry of the cruciate ligaments determines the condylar profile in the sagittal plane (O'Connor *et al.*, 1989). Overall, the cruciate ligaments ensures the anterior-posterior stability of the knee allowing flexion movements and while maintaining the articular surfaces in contact. Their function can be illustrated with a cross four-bar mechanism easy to visualize (Fig. 1a,1b and 1c), where the ACL and PCL are represented as links *cd* and *ab*, respectively. Meanwhile, the link *ad* represents the tibial link (fixed to the tibia), and *bc* represents the femoral link (fixed to the femur). Starting from the extended position (Fig. 1a), the ACL (*cd*) is uptight and is one of the limitings of the hyperextension. As a result, the flexion tilt the femoral link *bc* (Fig. 1b), whereas the LCP (*ab*) straightens up and the LCA (*cd*) is semi-recumbent. From the moment in which the flexion is between 70° (Fig. 1b) and 140° (Fig. 1c) the LCP straightens up almost vertically and tightens, but the ACL is semi-recumbent and distended (Kapandji *et al.*, 2000).

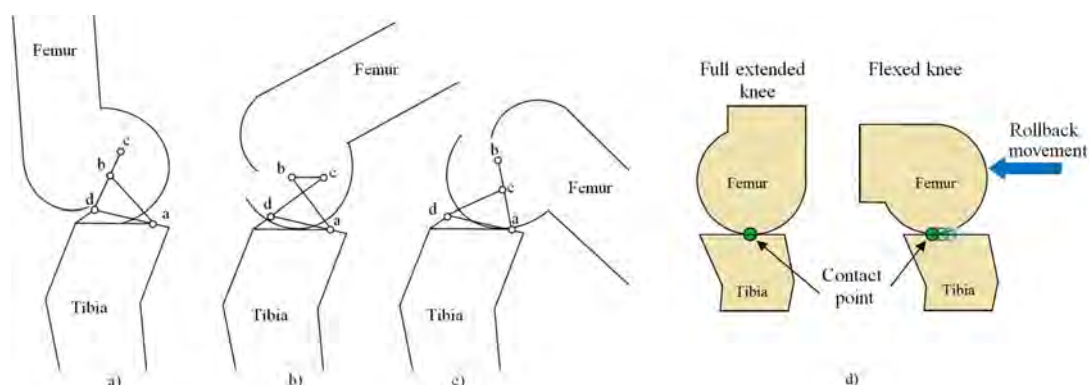


Figure 1. Mechanical model of the knee in flexion: a) 0° or fully extended, b) 70°, c) 140°, based on (O'Connor *et al.*, 1989), d) Rollback knee movement, Based on (Bacarim Pavan, 2010).

As shown in Figure 1, the femoral condyle is on the distal end of the femur, and it is articulated with the surface of the tibia, or the tibial plateau. The movement of the femoral condyles on the tibial surface combines *rolling* and *slip* (Kapandji *et al.*, 2000). During the first 30° of flexion, the femur *rolls* over the tibial surface (Bacarim Pavan, 2010), a phenomenon known as *rollback* (Fig. 1d), and in flexion angles higher to 30°, femoral condyles tend to maintain a fixed point of rotation of the tibial surface. The motion of *rolling* can be easily understood in terms of the operation of the cruciate ligaments, but the *slip* involves a higher complexity. The ligaments restrict movement of the femoral condyles so that they slide on the tibial surface in the opposite direction to its *rolling* (Kapandji *et al.*, 2000). During flexion, the ACL acts femur driving forward. Then, the ACL is responsible for the forward slip of the femoral condyle, associated with its *rolling* back. Viewed in this way, it can be said that the ACL is the main limiting of the anterior displacement of the tibia relative to the femur, or that it prevents the anterior tibial displacement. Another important function of the ACL is to limit the axial rotation of the femur on the tibia.

3. THEORETICAL FOUNDATIONS IN ROBOTICS

To perform a knee modeling based on the mechanisms theory, each anatomical knee structure should have a complete representation of the positions and forces that take place in the biomechanics of the joint.

For the static analysis, the Kirchhoff's **current law** adapted for mechanisms by Davies (Davies, 1981) can be used. To obtain the kinematic position of the ligaments, is used the Freudensteint's Equation (Freudenstein, 2010) and Rigid Transformations (Selig, 1992). Therefore, the position and orientation are entered in the Davies method. This allows to the kinematics and to the statics of a mechanism are able to be known by a unified methodology.

The use of the of Davies method is possible by previous knowledge of the Screw theory (Ball, 1900), which will also be reviewed in this session.

3.1 Davies method in static

The Kirchhoff's **Current Law** states that the algebraic sum of the currents entering and leaving a node is zero. In an analogous manner, to analysis of the static of mechanisms, Davies (1981) states that the sum of the wrench (screw of force) that belong to a same cut (performed in a subset of couplings) is zero, which is called the **Cut-Set Law**. Therefore, the method demonstrated in this session, uses Kirchhoff's laws to build the dependence of the unknowns. The physical characteristics such as force, moment, position, orientation and geometric characteristics, are included in the screw representation.

3.2 Screw theory

A screw is a geometric element defined by a directed line (axis) and an associated pitch h , which can be used to represent mechanical magnitudes (Campos *et al.*, 2005, 2009; Campos, 2004). It is said *normalized screw* $\hat{\$}$ when the directed line is represented by a normalized vector. The screw can be conveniently expressed through the six Plücker homogeneous coordinates, as shown in Eq. (1) where \vec{S} is the orientation vector along the helical axis, \vec{S}_0 is the position vector of any point of the helical axis relative to the origin of the system and $L, M, N, P^*, Q^* e R^*$ are the Plücker homogeneous coordinates (Campos *et al.*, 2005, 2009).

$$\hat{\$} = \left(\vec{S}; \vec{S}_0 \times \vec{S} + h\vec{S} \right)^T = (L, M, N; P^*, Q^*, R^*)^T \quad (1)$$

3.3 Screw in static

The state of forces of a rigid body relative to an inertial system can be described by a screw called wrench $\A , and consists of two main components: a moment \vec{T} parallel to the helical axis, and the resultant force vector \vec{R} , whose line of action defines the helical axis (Ball, 1900; Weihmann *et al.*, 2011a,b; Laus *et al.*, 2012). The moment \vec{T} has units of [force] x [length] equivalent to the product of the resultant force \vec{R} with the pitch h .

In a similar way to the homogeneous coordinates of Plücker (Eq. (1)), the wrench $\A can be rewritten with six coordinates, as shown in Eq. (2).

$$\$^A = (P^*, Q^*, R^*; L, M, N)^T = \left(\vec{S}_0 \times \vec{R} + h\vec{R}; \vec{R} \right)^T = \left(\vec{T}_P; \vec{R} \right)^T \quad (2)$$

The first three components of this vector correspond to the moment \vec{T}_P , and represents a free vector acting on the rigid body at a point P instantaneously coincident with the origin O . The resulting force \vec{R} is a row vector that acts on the screw axis (Weihmann *et al.*, 2011a,b; Laus *et al.*, 2012), and corresponds to the last three vector components of the Eq. (2).

Normalizing the wrench $\A , it is possible to separate it into a geometric element $\hat{\A , with no associated mechanical greatness, and a magnitude Ψ with force units, thus $\$^A = \hat{\$}^A \Psi$.

The wrench can assume two conditions according to the pitch value. When the pitch is zero $h=0$, the wrench represent purely force. When the screw has pitch $h = \infty$, means that the net force \vec{R} is zero and wrench represents purely moment. Thus, in a coupling each constraint is represented by a wrench (Weihmann *et al.*, 2011a,b; Laus *et al.*, 2012). Also, all brenc of a mechanism may be arranged in so-called *matrix of Actions*, which is denoted by $[A_D]_{\lambda \times C}$ shown in eq. (3), where C is the brute degree of restriction of the coupling network, equal to the sum of all unit restrictions c_p of each coupling belonging to the circuit of the mechanism. Normalizing the heliforças obtains the *Unit Action matrix* $[\hat{A}_D]_{\lambda \times C}$. For its part, the magnitudes arranged as a matrix, compose the *magnitude action vector* $\{\vec{\Psi}\}_{C \times 1}$.

The Davies **Cut-Set Law** states that the algebraic sum of the wrench that belong to the same cut (performed in a subset of couplings) is zero. Thus a cut in the λ space can be represented by the screw matrix notation as shown in Eq. (3):

$$\sum \$^A = [A_D]_{\lambda \times C} = [\hat{A}_D]_{\lambda \times C} \{\vec{\Psi}\}_{C \times 1} = \{\vec{0}\}_{\lambda \times 1} \quad (3)$$

In the same way for a number of k cuts, the system of the Eq.(3) is as follows:

$$[\hat{A}_N]_{\lambda, k \times C} \{\vec{\Psi}\}_{C \times 1} = \{\vec{0}\}_{\lambda, k \times 1} \quad (4)$$

Where $[\hat{A}_N]_{\lambda, k \times C}$ is called *Unit Network Action matrix*.

Authors such as Weihmann *et al.* (2011a,b); Laus *et al.* (2012) show clearly how to set the system of the Eq. (3), taking into account the graphs that determine the topological relation of the mechanism. The solution of the Eq. (3) depends on the proper selection of C_N primary variables belonging to the vector $\{\vec{\Psi}\}_{C \times 1}$, which are usually related to the actuators, through external forces that were internalized. This equation system can be partitioned between C_N primary variables and secondary variables a , where the secondary variables lead the sub-index S and the primary variables carry the subscript P . The last step is to isolate the unknowns vector $\{\Psi_S\}_{a \times 1}$, resulting in the static solution:

$$\{\vec{\Psi}_S\}_{a \times 1} = -[\hat{A}_{NS}]_{a \times a}^{-1} [\hat{A}_{NP}]_{a \times C_N} \{\vec{\Psi}_P\}_{C_N \times 1} \quad (5)$$

Where $[\hat{A}_{NS}]$ is the *Secondary Network submatrix* and $[\hat{A}_{NP}]$ is the *Primary Network submatrix*. Assigning values to the primary variables $[\vec{\Psi}_P]$ is possible to obtain a static solution, corresponding to the Eq. (5).

4. PROPOSED METHODOLOGY

The proposed methodology for modeling the knee in the sagittal plane provides a unique and systematic approach for the biomechanical analysis of the knee, and it consists of four steps (Fig. 2): (1) Schematic representation of the physical model of the knee, (2) Identification of the successive positions of the cruciate ligaments, (3) Determining the cruciates ligaments forces, and (4) Consideration of elastic behavior.

The first step identifies the initial positions of the cruciate ligaments when the knee is in full extension position, based on magnetic resonance imaging (MRI). The second step leads to the identifications of the successive positions of the cruciate ligaments in the flexion-extension movement of the knee. The third step leads to the identification of the forces acting on the cruciate ligaments for each position, by means of the Davies method. This static analysis enables to obtain the *In-Situ* force of the ACL (or ACL graft) and the magnitude of pre-tension of the ACL graft fixation, due to an applied external load. The fourth step leads to the identification of forces and displacements considering elastic behavior of the cruciate ligaments. This is performed with the *In-Situ* force, obtained in the previous step, and an experimental stiffness constant k , obtained from Górios *et al.* (2001). Finally, it can be analyzed the effect of considering the elastic behavior. This whole procedure is briefly schematized in the Fig. 2 and it will be explained in detail below.

4.1 Schematic representation of the physical model of the knee in the sagittal plane

The proposed physical model is based on the experimental approach presented by O'connor *et al.* (1989), where it is considered that the cruciate ligaments are always in tension and a cross four-bar mechanism $abcd$ is superimposed to the cruciate ligaments, as shown in Fig. 3a. Here, a , b , c and d are rotary joints of the mechanism, the link ab represents the PCL, the link cd represents the ACL, the link ad represents the tibial link (fixed to the tibia), and bc represents the femoral link (fixed to the femur). The angle α indicates the orientation of the link cd relative to the tibial link, and β is the orientation angle of the link ab relative to the tibial link. I is the intersection of the cruciate ligaments and represents the center of rotation of the joint.

The length and position of the links in the proposed model, depend on the ACL and PCL length, as well as the location of the ligament insertions on the tibia and femur. The determination of these parameters can be performed by MRI inspection as shown in Fig. 3b.

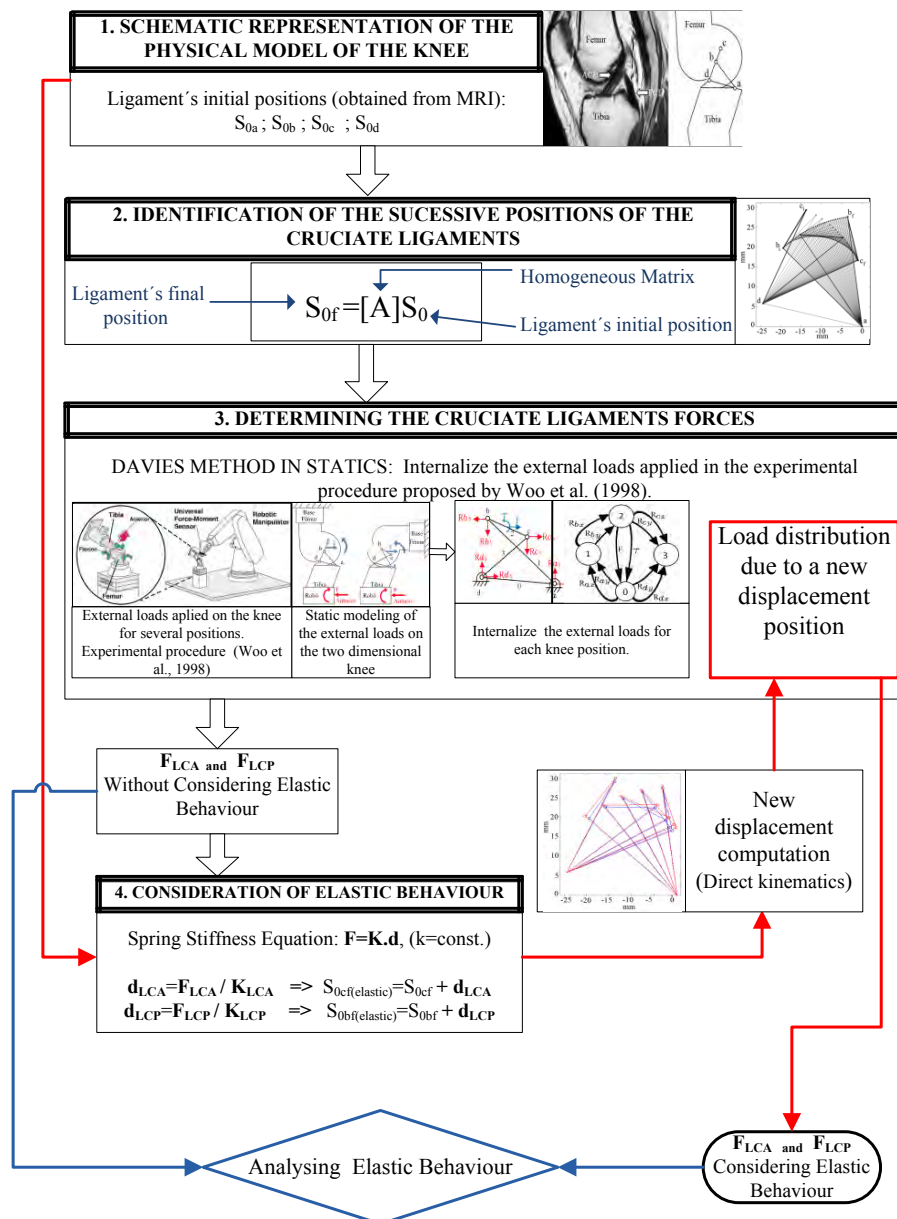


Figure 2. Schematic process of the proposed methodology, composed by four steps: (1) Schematic representation of the physical model of the knee, (2) Identification of the successive positions of the cruciate ligaments, (3) Determining the cruciate ligaments forces, and (4) Consideration of elastic behavior.

Williams *et al.* (1991) did an exhaustive literature review, which showed the wide range of variation of the lengths of the cruciate ligaments in the sagittal plane, indicating that the length of the ACL and the PCL varies between 23 and 40 mm. Authors such as Bradley *et al.* (1988); Clement *et al.* (1989); Crowninshield *et al.* (1976) and Wang *et al.* (1973) also present studies with ligament length values. The ligament length values chosen for the simulation of the proposed model were based on the most frequent values found in the literature, out of which: LCA (cd)=24.6mm, LCP (ab)=25.7mm, femoral link (bc)=13mm, tibial link (ad)=22mm.

4.2 Identification of the successive positions of the cruciate ligaments

In this section, the successive positions of the cruciate ligaments are calculated, from the maximum extension up to the maximum flexion of the knee ($0^\circ - 140^\circ$), as shown in Fig.1. For this analysis, the Freudenstein's equation (Freudenstein, 2010) and Rigid Transformations (Selig, 1992) are used. The Freudenstein's equation (Freudenstein, 2010) is widely used for the synthesis of 4-bar mechanisms, and in the proposed model it allows to find the β angle in function of α angle (Fig. 3a).

Considering the fixed points a and d , and the point a as the origin of the coordinate system, the successive positions

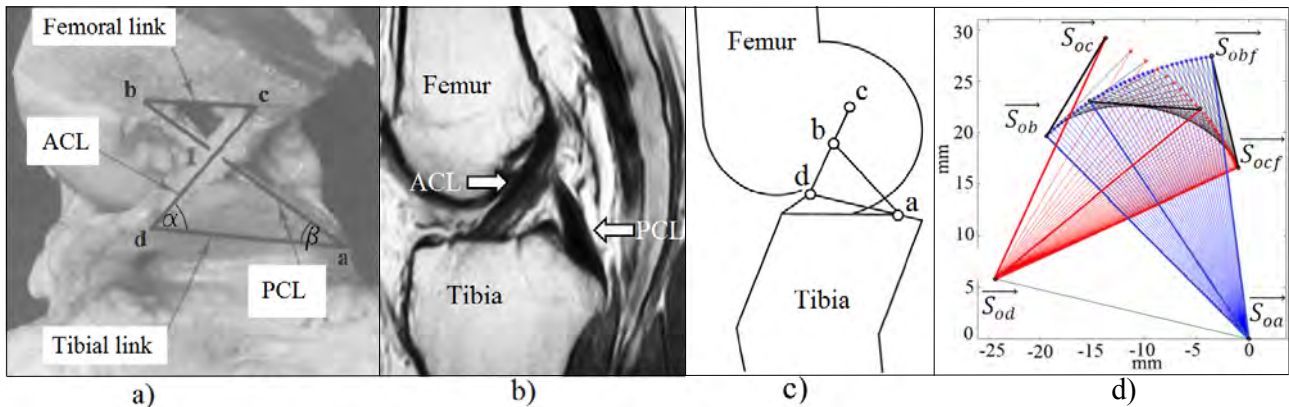


Figure 3. a) Knee in flexion with a cross four-bar mechanism superimposed on the cruciate ligaments (O'Connor *et al.*, 1989). b) MRI of a knee in extension (Lykissas *et al.*, 2010). c) Physical model of the knee in extension (O'Connor *et al.*, 1989). d) Successive positions of the cruciate ligaments: ACL in red, LCP in blue, tibial and femoral link in black.

of the links ab and cd can be described. The position of the vector ab is described as the rotation of the point b around the point a , as shown in equation 6, whereas \vec{S}_{obf} is the final position of the point b , \vec{S}_{ob} is the initial position of the point b , and $[A_\beta]$ is homogeneous matrix that describes the rotation angle β around the point a .

$$\vec{S}_{obf} = [A_\beta] \vec{S}_{ob} \quad (6)$$

In the same way, the position vector cd is described as the rotating point c around the point d , as shown in equation 7, whereas \vec{S}_{ocf} is the final position of the point c , \vec{S}_{oc} is the initial position of the point c , and $[A_\alpha]$ is the homogeneous matrix that describes the rotation angle α around the point d .

$$\vec{S}_{ocf} = [A_\alpha] \vec{S}_{oc} \quad (7)$$

Entering the successive values of α (from the maximum extension up to the maximum flexion) in the Eq.(6) and (7), all positions of the cruciate ligaments are obtained, as shown in Fig. 3d.

4.3 Determining the cruciates ligaments forces

In this section the forces in the cruciate ligaments are calculated by static analysis using the the Davies **Cut-Set Law** (Davies, 1981). For this, the experimental procedure proposed by Woo *et al.* (1998) is modeled and simulated to obtain the *In-Situ* force by using a robotic manipulator system (Unimate, PUMA model 762) and a universal force-moment sensor UFS (JR3, model 4015), as shown in Fig. 4a. This experimental procedure is described as follows. Woo *et al.* (1998) analyzed the *In Situ* force in the ACL, using knees specimens whose tibia and femur were cut to a length of 200mm from the joint line, secured within thick-walled aluminum cylinders and rigidly fixed. The cylinder that holds the femur is fixed to the ground by a supportive base structure. The cylinder that holds the tibia is fixed to the UFS, which in turn is fixed on the end-effector of the robot (Fig.4a). To obtain the *In-Situ* force of the ACL, the robot applies an anterior tibial load as shown by the red arrow in Fig. 4a, and it is applied in five knee angles of flexion (0° , 15° , 30° , 60° , 90°).

The load direction is chosen anteriorly to the tibia because there are exams, where the doctor manually applies a similar load on the tibia in order to determine the existence of ACL injuries (Drawer Test, Lachman test). A second reason, because the ACL is the primary limiter of anterior displacement of the tibia relative to the femur. Therefore, the load applied by the robot directly affects the LCA. For its part, the UFS sensor allows to save the data of force and torque that occur in the tibia, and by *Jacobian* operations, the magnitudes that occur in the LCA are known, such as the *In-Situ* force (Woo *et al.*, 1998, 2006b, 2004, 2006a).

The modeling of the experimental procedure of Woo *et al.* (1998) is shown in Fig. 4b. This model adopts the inertial reference system coinciding with the point a , belonging to the tibia. This convention considers that the femur is moving and the tibia is fixed.

The anterior tibial force applied by the robot has a magnitude of F_1 , and is accompanied by a torque τ_1 that constrains the flexion angle in order to provoke a forward translation of the tibia relative to the femur. The loads applied by the robot are shown in red (Fig. 4b). Whereas the ligaments transmit the applied loads by the robot, from the tibia to the femur, in the form of a reaction force F and a torque reaction τ , shown in blue (Fig. 4b). The reaction force F keeps constant its direction throughout of the knee flexion, and it is considered to be located at the midpoint of the femoral link bc . The application point of the force (F) is called \vec{S}_{0F} .

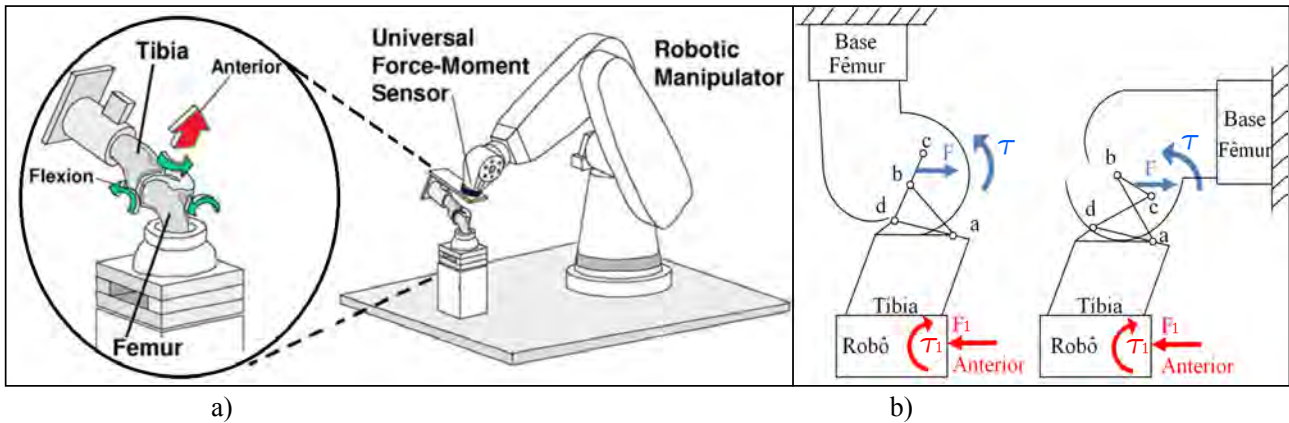


Figure 4. a) Experimental procedure proposed by Woo *et al.* (1998). b) Static modeling of the experimental procedure (Saldías *et al.*, 2013).

For the static analysis by Davies method (Davies, 1981), both external force and torque shown in red (Fig. 4b), must be internalized and replaced with equivalent actions between links belonging to the analyzed mechanism, resulting in a *over-constrained* chain (Fig. 5a). At this stage, numbers are assigned to each link and internal actions R_x and R_y are specified at each joint, as well as the force F and torque τ (Fig. 5a).

Once the actions are internalized, the action graph G_A (Fig.5b) is formed, where the 8 edges R_x and R_y represent the passive actions between each link in 0, 1, 2 e 3, and the edges F and τ represent the active actions between the links 0 and 2.

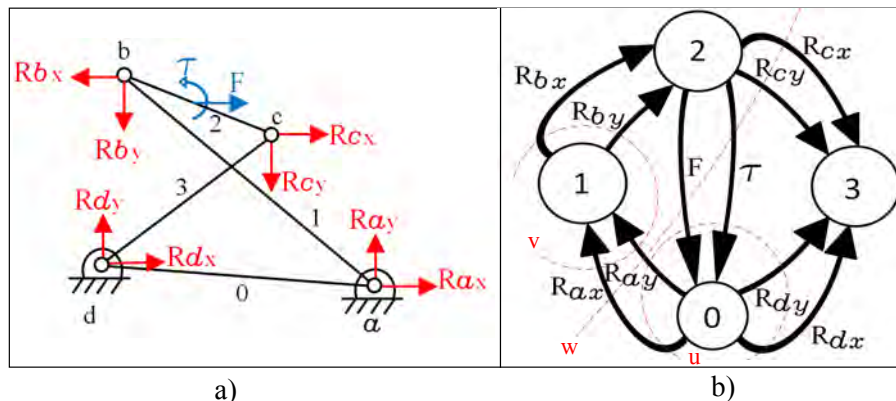


Figure 5. a) Actions on the couplings of the modeled mechanism. b) Action graph G_A of the modeled mechanism, and k cuts in red dashed lines. (Saldías *et al.*, 2013).

For the graph G_A the k cuts are determined. The number of k cuts is given by the relation 8, (Tsai, 2001):

$$k = n - 1 = 4 - 1 = 3 \quad (8)$$

Where n is the number of vertices of the graph G_A . Based on the generator tree (Weihmann *et al.*, 2011a,b; Laus *et al.*, 2012), it is determined where the $k = 3$ cuts in the graph will be applied. The 3 cuts are called u , v and w , and are shown in red dashed lines (Fig. 5b).

For the internalized actions chain, in the workspace $\lambda = 3$, can be described $\lambda \cdot k$ equations that must be satisfied by C unknowns. The C unknowns correspond to the sum of the number of passive actions R_x and R_y , and active actions F e τ :

$$C = R_x + R_y + F + \tau = 4 + 4 + 1 + 1 = 10 \quad (9)$$

These C unknowns can be written as a function of C_N primary variables (Weihmann *et al.*, 2011a,b; Laus *et al.*, 2012).

$$C_N = C - \lambda \cdot k = 10 - (3 \cdot 3) = 1 \quad (10)$$

Thus, it is possible to determine the internal actions C of the chain, by imposing $C_N = 1$ variables, corresponding to the force F .

In relation to wrench to the rotary joints (R_x and R_y), and the force F pitch h is zero, therefore wrenches are obtained that represent pure force constraints as shown in eq.11.

$$\$_ = \left(\vec{S}_0 \times \vec{S}; \vec{S} \right)^T = \left(\vec{S}_0 \times \vec{R}; \vec{R} \right)^T \quad (11)$$

On the other hand, the wrench pitch corresponding to pure torque τ is infinite; therefore, wrenches which represent pure torque are obtained as indicated in equation 12.

$$\$_ = \left(\vec{S}; \vec{0} \right)^T = \left(\tau; \vec{0} \right)^T \quad (12)$$

Considering the eq.(11) and Eq. (12), and that the position vectors \vec{S}_0 of the wrenches are obtained in the step 2 of the methodology (Identification of the successive positions of the cruciate ligaments), the following wrenches are obtained for the proposed model:

$$\begin{aligned} \$_{a_x} &= \begin{pmatrix} \vec{0} \\ \vec{R}_{a_x} \end{pmatrix}; \$_{a_y} = \begin{pmatrix} \vec{0} \\ \vec{R}_{a_y} \end{pmatrix}; \$_{b_x} = \begin{pmatrix} \vec{S}_{0b_f} \times \vec{R}_{b_x} \\ \vec{R}_{b_x} \end{pmatrix}; \$_{b_y} = \begin{pmatrix} \vec{S}_{0b_f} \times \vec{R}_{b_y} \\ \vec{R}_{b_y} \end{pmatrix}; \\ \$_{c_x} &= \begin{pmatrix} \vec{S}_{0c_f} \times \vec{R}_{c_x} \\ \vec{R}_{c_x} \end{pmatrix}; \$_{c_y} = \begin{pmatrix} \vec{S}_{0c_f} \times \vec{R}_{c_y} \\ \vec{R}_{c_y} \end{pmatrix}; \$_{d_x} = \begin{pmatrix} \vec{S}_{0d_f} \times \vec{R}_{d_x} \\ \vec{R}_{d_x} \end{pmatrix}; \\ \$_{d_y} &= \begin{pmatrix} \vec{S}_{0d_f} \times \vec{R}_{d_y} \\ \vec{R}_{d_y} \end{pmatrix}; \$_F = \begin{pmatrix} \vec{S}_{0F} \times \vec{F} \\ \vec{F} \end{pmatrix}; \$_\tau = \begin{pmatrix} \vec{\tau} \\ \vec{0} \end{pmatrix}; \end{aligned} \quad (13)$$

The Davies **Cut-Set Law** (Davies, 1981) states that the sum of the wrenches belonging to a cut is zero (Eq.4). To apply the **Cut-Set Law** it is built the *Unit Network Action matrix* $[\hat{A}_N]_{\lambda,k \times C}$. In this matrix, the normalized wrenches belonging to each cut u , v and w of the graph G_A are placed in an organized way, (Fig. 5b). The *Unit Network Action matrix* for the proposed model is presented in Eq. (14):

$$\begin{array}{l} \text{cut } u \\ \text{cut } v \\ \text{cut } w \end{array} \begin{bmatrix} \hat{\$_}_{a_x} & \hat{\$_}_{a_y} & \vec{0} & \vec{0} & \vec{0} & \vec{0} & \hat{\$_}_{d_x} & \hat{\$_}_{d_y} & \hat{\$_}_\tau & \hat{\$_}_F \\ \hat{\$_}_{a_x} & \hat{\$_}_{a_y} & \hat{\$_}_{b_x} & \hat{\$_}_{b_y} & \vec{0} & \vec{0} & \vec{0} & \vec{0} & \vec{0} & \vec{0} \\ \hat{\$_}_{a_x} & \hat{\$_}_{a_y} & \vec{0} & \vec{0} & \hat{\$_}_{c_x} & \hat{\$_}_{c_y} & \vec{0} & \vec{0} & \hat{\$_}_\tau & \hat{\$_}_F \end{bmatrix} = [\hat{A}_N]_{\lambda,k \times C} \quad (14)$$

Thus, the Eq. (4) applied to the proposed model becomes:

$$\begin{bmatrix} \hat{\$_}_{a_x} & \hat{\$_}_{a_y} & \vec{0} & \vec{0} & \vec{0} & \vec{0} & \hat{\$_}_{d_x} & \hat{\$_}_{d_y} & \hat{\$_}_\tau & \hat{\$_}_F \\ \hat{\$_}_{a_x} & \hat{\$_}_{a_y} & \hat{\$_}_{b_x} & \hat{\$_}_{b_y} & \vec{0} & \vec{0} & \vec{0} & \vec{0} & \vec{0} & \vec{0} \\ \hat{\$_}_{a_x} & \hat{\$_}_{a_y} & \vec{0} & \vec{0} & \hat{\$_}_{c_x} & \hat{\$_}_{c_y} & \vec{0} & \vec{0} & \hat{\$_}_\tau & \hat{\$_}_F \end{bmatrix}_{9 \times 10} = \begin{bmatrix} R_{a_x} \\ R_{a_y} \\ R_{b_x} \\ R_{b_y} \\ R_{c_x} \\ R_{c_y} \\ R_{d_x} \\ R_{d_y} \\ \tau \\ F \end{bmatrix}_{10 \times 1} = [\vec{0}]_{10 \times 1} \quad (15)$$

According to the Eq. (5), the system of the Eq. (15) can be rewritten, so that the *Primary Network submatrix* $[\hat{A}_{NP}]$ is equal to the last column of the matrix $[\hat{A}_N]_{\lambda,k \times C}$, and *Secondary Network submatrix* $[\hat{A}_{NS}]$ is equal to the first nine columns of the matrix $[\hat{A}_N]_{\lambda,k \times C}$. Since $[\hat{A}_{NS}]$ is invertible, the magnitudes of secondary actions $[\vec{\Psi}_S]$ are calculated by:

$$\begin{bmatrix} R_{a_x} \\ R_{a_y} \\ R_{b_x} \\ R_{b_y} \\ R_{c_x} \\ R_{c_y} \\ R_{d_x} \\ R_{d_y} \\ \tau \end{bmatrix}_{9 \times 1} = - \begin{bmatrix} \hat{\$_}_{a_x} & \hat{\$_}_{a_y} & \vec{0} & \vec{0} & \vec{0} & \vec{0} & \hat{\$_}_{d_x} & \hat{\$_}_{d_y} & \hat{\$_}_\tau \\ \hat{\$_}_{a_x} & \hat{\$_}_{a_y} & \hat{\$_}_{b_x} & \hat{\$_}_{b_y} & \vec{0} & \vec{0} & \vec{0} & \vec{0} & \vec{0} \\ \hat{\$_}_{a_x} & \hat{\$_}_{a_y} & \vec{0} & \vec{0} & \hat{\$_}_{c_x} & \hat{\$_}_{c_y} & \vec{0} & \vec{0} & \hat{\$_}_\tau \end{bmatrix}_{9 \times 9}^{-1} \begin{bmatrix} \hat{\$_}_F \\ \vec{0} \\ \hat{\$_}_F \end{bmatrix}_{9 \times 1} \cdot \vec{F} \quad (16)$$

Assigning a value to the primary variable \vec{F} , it is possible to obtain a static solution, corresponding to the Eq. (16). In order to perform the static simulation that represents the experimental procedure proposed by Woo *et al.* (1998), the motion of the knee flexion ranges from 0° to 90° . For each flexion angle, an anterior tibial force \vec{F} is applied. The *In-Situ* force of *LCA* is calculated as the force that passes through the link *dc* for each flexion angle, that is: $F_{LCA\text{insitu}}=R_{dx}/(\cos(\alpha))$. The *In-Situ* force of *LCP* is calculated as the force that passes through the link *ab* for each flexion angle, that is: $F_{LCP\text{insitu}}=R_{ax}/(\cos(\beta))$.

4.4 Consideration of elastic behavior

This step leads to the identification of forces and displacements of the cruciate ligaments considering elastic behavior. The elastic displacements of the ligaments *d* are obtained by means of the *Spring Stiffness Equation*, shown in Eq. (17). There, *K* is the stiffness constant, *F* is the value corresponding to the *In-Situ* force of the cruciate ligaments, which had been obtained for each flexion angle in the previous step of the methodology (Fig. 2).

$$F = K.d \quad (17)$$

Specifically, the elastic displacements of the *ACL* and *PCL* were obtained as shown in Eq. (18), where $K_{ACL}=121.91N/mm$ and $K_{PCL}=143.88N/mm$ are the constant values of *ACL* and *PCL* stiffness, proposed by Górios *et al.* (2001).

$$\begin{aligned} d_{ACL} &= F_{ACL}/K_{ACL} \\ d_{PCL} &= F_{PCL}/K_{PCL} \end{aligned} \quad (18)$$

It is important to note that each elastic displacement (d_{ACL} and d_{PCL}) varies as long as the *In-Situ* force varies for each angle flexion. All the successive ligaments positions had to be updated, as shown in Eq. (19) considering these elastic displacements. The updated positions of the *ACL* and *PCL*, now considering elastic behavior, are called $\vec{S}ocf_{(elastic)}$ and $\vec{S}obf_{(elastic)}$ respectively. Three principal successive positions of the cruciate ligaments, considering elastic behavior (red) and disconsidering elastic behavior (blue), are shown in (Fig. 6)

$$\begin{aligned} \vec{S}ocf_{(elastic)} &= \vec{S}ocf + d_{ACL} \\ \vec{S}obf_{(elastic)} &= \vec{S}obf + d_{PCL} \end{aligned} \quad (19)$$

For the updated positions the **Cut-Set Law** is reapplied, finding forces that consider elastic behavior of the cruciate ligaments, and they will be shown in the next section.

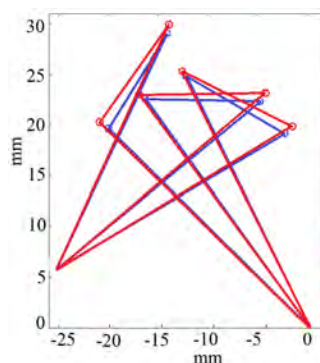


Figure 6. Positions of the cruciate ligaments: considering elastic behavior (red) and disconsidering elastic behavior (blue).

5. RESULTS

In this section, the results of the *In-Situ* forces in the *ACL* and the anterior tibial displacement simulated in the model are presented. To validate the proposed model, the experimental results obtained by Woo *et al.* (1998) are compared with the two simulated results: one that considers elastic behavior, and another that disconsiders elastic behavior. The experimental values (force and displacement) were obtained when Woo *et al.* (1998) robotically applied an anterior tibial load $F_1 = 110N$ for the following flexion angles: 0° , 15° , 30° , 60° , 90° . On the other hand, the simulated results are obtained considering that F_1 is continuously applied from 0° up to 90° .

The results of the *In-Situ* forces in the ACL, are shown in Fig. 7a. The experimental values are shown in blue triangles. The simulated values that consider elastic behavior are shown in black squares. The simulated values that disconsider elastic behavior are shown in red circles. The experimental values of *In-Situ* force grow from 0° up to 15° of flexion, after these angle the values are decreasing. The simulated values of *In-Situ* force start to decrease from 0° up to 90°. The maximum difference between experimental and simulated values of *In-Situ* force is 20.7N at 0° of flexion, while the minimum differences (colse to 0N) are from 12° up to 90° of flexion. The difference between the two simulated results, one that considers and another that disconsiders elastic behavior, vary within 3.0N and 3.7N. Of which, those that consider elastic behavior are slightly higher.

The anterior tibial displacement due to the anterior tibial load $F_1 = 110\text{N}$, are shown in Fig. 7b. The experimental values are shown in blue triangles. The simulated values that consider elastic behavior are shown in black squares. The simulated values that disconsider elastic behavior are shown in red asterisks. The experimental values of anterior tibial displacement grows strongly from 0° up to 30° of flexion (*rollback* effect). After that, the displacement decreases. This means that the femur glides over the tibia and even changes the direction of displacement. The simulated values of anterior tibial displacement start to grow continuously from 0°, without changing its direction. The maximum difference between experimental and simulated values of anterior tibial displacement is 4.9mm at 0° of flexion, while the minimum differences (0mm) are located at 67° and 70° of flexion. The difference between two simulated results, one that considers and another that disconsiders elastic behavior, vary within 0.2mm and 0.9mm. Of which, those that consider elastic behavior are slightly higher.

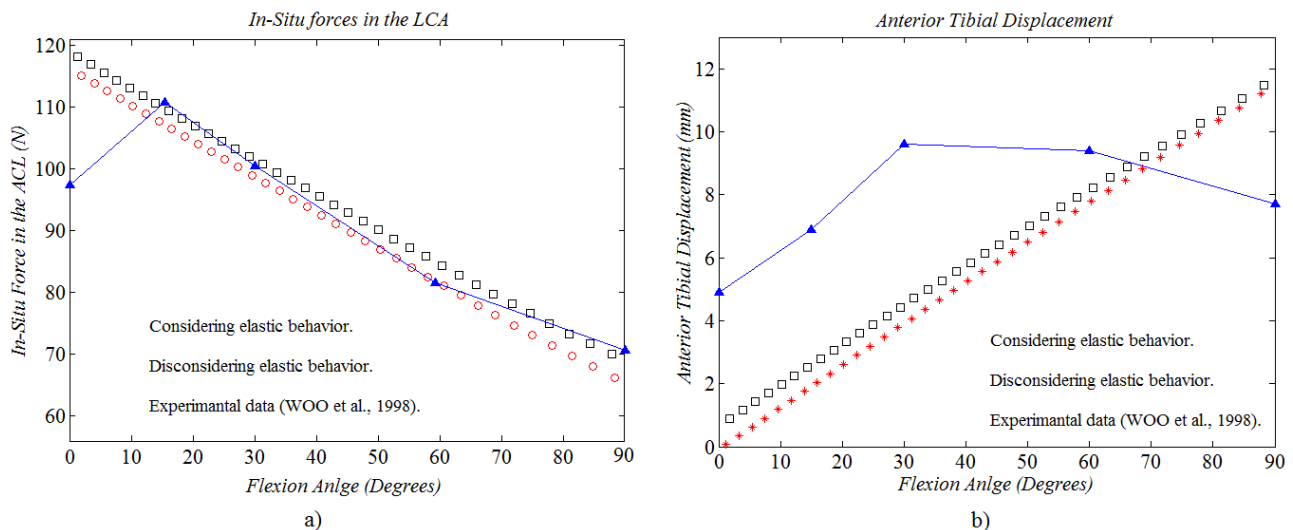


Figure 7. Experimental values, simulated values that consider elastic behavior, and simulated values that do not consider elastic behavior for: a) *In-Situ* forces in the ACL. b) Anterior tibial translation.

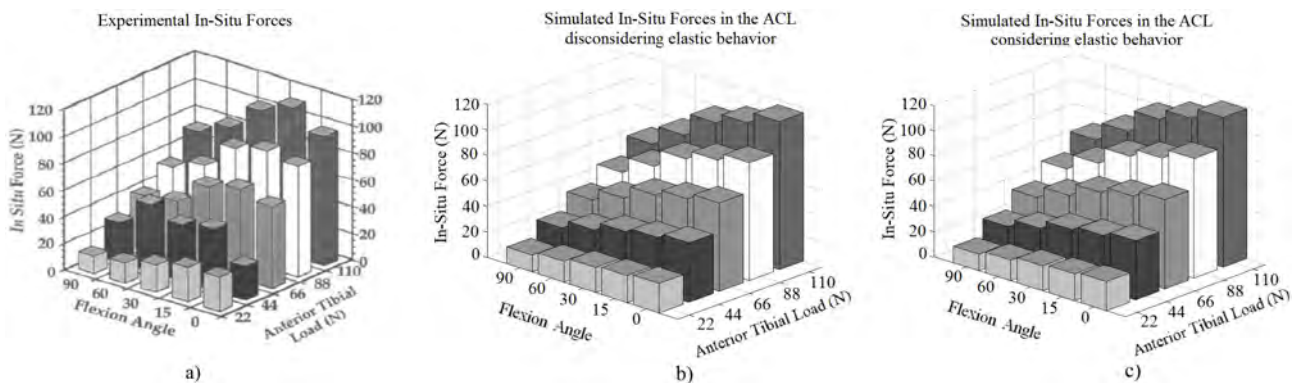


Figure 8. *In-Situ* Forces for F_1 magnitudes: a) Experimental values (Woo *et al.*, 1998), b) simulated values that disconsider elastic behavior, and c) Simulated values that consider elastic behavior.

After that procedure, the *In-Situ* forces in the ACL were evaluated on the same flexion angles, but varying the magnitude of the anterior tibial forces F_1 to: 110N, 88N, 66N, 44N and 22N. The experimental values are shown in Fig.8a. The

simulated values that disconsider elastic behavior are shown in Fig.8b. The simulated values that consider elastic behavior are shown in Fig.8c. In Fig.8a can be seen that the graphs of experimental results of *In-Situ* forces have a convex shape with the maximum values close to 15° of flexion. In contrast, the simulated values of forces (Fig.8a,b) have a decreasing shape with a maximum at 0° of flexion. The maximum difference between experimental and simulated values of *In-Situ* forces is 20.7N at 0° of flexion. The maximum difference between simulated values of *In-Situ* forces, that consider and disconsider elastic behavior, is 3.7N at 90° of flexion.

6. CONCLUSIONS

The proposed model of the human knee joint allows to obtain results of position and *In-Situ* forces in the ACL close to the experimental ones. This fact makes possible to provide support to the orthopedic surgeons with important informations for preoperative planning and medical decision making.

The inclusion of the elastic behavior can be negligible, because the largest error between simulated *In-Situ* forces, that consider and disconsider elastic behavior, is small (5,1%). In its turn, the largest error between the simulated anterior tibial displacements, that consider and disconsider elastic behavior, is small as well (6.1%). It is concluded that a model with fixed-length links would reproduce results close the experimental ones.

The proposed methodology for inclusion of the elastic behavior could be considered as a series of iterations, where the positions of the ligaments are accommodating until converge, according to an external load F_1 and a stiffness constant K . But in this work a single iteration has been performed, because the variation of the length of the ligaments in one iteration resulted very small, thus considering it as already converged.

The main reason of the difference between simulated and experimental results of *In-Situ* forces in the ACL is the disregarding of the three-dimensional effects, such as axial rotation of the knee, which occurs strongly in the first degrees of knee flexion, but also on the whole knee movement. For the same reason, the simulated values of anterior tibial displacement are growing continuously without change of direction (unlike the experimental values). Although the results of this study are encouraging, they still do not reflect faithfully the experimental results.

The proposed methodology would allow to improve the present model, simulating customized models of the knee, including three dimensional effects and other internal structures, that will allow better results and closer to the experimental ones.

7. REFERENCES

- Bacarim Pavan, R., 2010. "Análise dinâmica de corpos rígidos aplicada ao projeto de uma prótese para artroplastia total de joelho".
- Ball, S., 1900. *A Treatise on the Theory of Screws*. Cambridge Univ Pr.
- Bradley, J., Fitzpatrick, D., Daniel, D., Shercliff, T. and O'Connor, J., 1988. "Orientation of the cruciate ligament in the sagittal plane. a method of predicting its length-change with flexion". *Journal of Bone and Joint Surgery-British Volume*, Vol. 70, No. 1, p. 94.
- Campos, A., 2004. *Cinemática diferencial de manipuladores empregando cadeias virtuais*. Ph.D. thesis, Ph. D. Thesis.
- Campos, A., Guenther, R. and Martins, D., 2005. "Differential kinematics of serial manipulators using virtual chains". *Journal of the Brazilian Society of Mechanical Sciences and Engineering*, Vol. 27, p. 345.
- Campos, A., Guenther, R. and Martins, D., 2009. "Differential kinematics of parallel manipulators using assur virtual chains". *Proceedings of the Institution of Mechanical Engineers, Part C: Journal of Mechanical Engineering Science*, Vol. 223, No. 7, p. 1697.
- Clement, B., Drouin, G., Shorrock, G. and Gely, P., 1989. "Statistical analysis of knee ligament lengths". *Journal of biomechanics*, Vol. 22, No. 8-9, pp. 767-774.
- Crowninshield, R., Pope, M. and Johnson, R., 1976. "An analytical model of the knee". *Journal of Biomechanics*, Vol. 9, No. 6, pp. 397-405.
- Davies, T., 1981. "Kirchhoff's circulation law applied to multi-loop kinematic chains". *Mechanism and machine theory*, Vol. 16, No. 3, pp. 171-183.
- Freudenstein, F., 2010. "Approximate synthesis of four-bar linkages". *Resonance*, Vol. 15, pp. 740-767. ISSN 0971-8044. URL <http://dx.doi.org/10.1007/s12045-010-0084-7>. 10.1007/s12045-010-0084-7.
- Górios, C., Hernandez, A.J., Amatuzzi, M.M., Leivas, T.P., Pereira, C.A.M., NETO, R.B. and Pereira, E.d.S., 2001. "Estudo da rigidez do ligamento cruzado anterior do joelho e dos enxertos para sua reconstrução com o ligamento patelar e com os tendões dos músculos semitendíneo e grácil". *Acta Ortop Bras*, Vol. 9, No. 2, p. 26.
- Gregorio, R. and Parenti-Castelli, V., 2006. "Parallel mechanisms for knee orthoses with selective recovery action". *Advances in Robot Kinematics*, pp. 167-176.
- Huson, A., Spoor, C. and Verbout, A., 1989. "A model of the human knee, derived from kinematic principles and its relevance for endoprosthesis design". *Acta Morphologica Neerlandica-Scandinavica*, Vol. 27, pp. 45-62.
- Kapandji, A. et al., 2000. *Fisiologia articular*. Editorial Médica Panamericana.

- Laus, L., Simas, H., CRUZ, D. and Martins, D., 2012. "Efficiency of gear trains determined using graph and screw theories". *Mechanism and Machine Theory*, Vol. 1. doi:10.1016/j.mechmachtheory.2012.01.011. URL http://authors.elsevier.com/TrackPaper.html?trk_article=MAMT1944trk_surname=Laus.
- Lykissas, M., Mataliotakis, G., Paschos, N., Panovrakos, C., Beris, A. and Papageorgiou, C., 2010. "Simultaneous bi-compartmental bucket-handle meniscal tears with intact anterior cruciate ligament: a case report". *Journal of medical case reports*, Vol. 4, No. 1, pp. 1–4.
- O'Connor, J., Shercliff, T., Biden, E. and Goodfellow, J., 1989. "The geometry of the knee in the sagittal plane". *ARCHIVE: Proceedings of the Institution of Mechanical Engineers, Part H: Journal of Engineering in Medicine 1989-1996 (vols 203-210)*, Vol. 203, No. 48, pp. 223–233.
- Olanlokun, K. and Wills, D., 2002. "A spatial model of the knee for the preoperative planning of knee surgery". *Proceedings of the Institution of Mechanical Engineers, Part H: Journal of Engineering in Medicine*, Vol. 216, No. 1, p. 63.
- Ottoboni, A., Parenti-Castelli, V. and Leardini, A., 2005. "On the limits of the articular surface approximation of the human knee passive motion models". In *Proceedings of the 17th AIMETA Congress of Theoretical and Applied Mechanics, Firenze, Italy*.
- Parenti-Castelli, V., Leardini, A., Di Gregorio, R. and O'Connor, J., 2004. "On the modeling of passive motion of the human knee joint by means of equivalent planar and spatial parallel mechanisms". *Autonomous Robots*, Vol. 16, No. 2, pp. 219–232.
- Saldias, D.A.P., de Mello Roesler, C.R. and Martins, D., 2013. "A human knee joint model based on screw theory and its relevance for preoperative planning". *Mecánica Computacional, Volume XXXI. Number 24. Computational Modeling in Bioengineering and Biomedical Systems (B)*, pp. 3847–3871.
- Sancisi, N. and Parenti-Castelli, V., 2011a. "A novel 3d parallel mechanism for the passive motion simulation of the patella-femur-tibia complex". *Meccanica*, pp. 1–14.
- Sancisi, N. and Parenti-Castelli, V., 2011b. "A sequentially-defined stiffness model of the knee". *Mechanism and Machine Theory*.
- Sancisi, N., Zannoli, D., Parenti-Castelli, V., Belvedere, C. and Leardini, A., 2011. "A one-degree-of-freedom spherical mechanism for human knee joint modelling". *Proceedings of the Institution of Mechanical Engineers, Part H: Journal of Engineering in Medicine*, Vol. 225, No. 8, pp. 725–735.
- Sancisi, N. and Parenti-Castelli, V., 2010. "A 1 dof parallel spherical wrist for the modelling of the knee passive motion". *Mechanism and Machine Theory*, Vol. 45, No. 3, pp. 658–665.
- Selig, J., 1992. *Introductory robotics*. Prentice Hall.
- Tsai, L., 2001. *Mechanism design: enumeration of kinematic structures according to function*, Vol. 16. CRC.
- Wang, C., Walker, P. and Wolf, B., 1973. "The effects of flexion and rotation on the length patterns of the ligaments of the knee". *Journal of biomechanics*, Vol. 6, No. 6, pp. 587–592.
- Weihmann, L., Martins, D., Bernert, D.L.A. and Coelho, L.d.S., 2011a. "Optimization of planar parallel manipulators force capabilities using improved harmony search approach." In *21st International Congress of Mechanical Engineering - COBEM, 2011, Natal. Proceedings of the 21st International Congress of Mechanical Engineering*.
- Weihmann, L., Martins, D. and dos Santos Coelho, L., 2011b. "Modified differential evolution approach for optimization of planar parallel manipulators force capabilities". *Expert Systems with Applications*.
- Williams, P., Peura, G. and Hoffman, A., 1991. "A model of knee motion in the sagittal plane". In *Bioengineering Conference, 1991., Proceedings of the 1991 IEEE Seventeenth Annual Northeast*. IEEE, pp. 273–274.
- Wilson, D., Feikes, J. and O'Connor, J., 1998. "Ligaments and articular contact guide passive knee flexion". *Journal of biomechanics*, Vol. 31, No. 12, pp. 1127–1136.
- Wilson, D. and O'Connor, J., 1997. "A three-dimensional geometric model of the knee for the study of joint forces in gait". *Gait & Posture*, Vol. 5, No. 2, pp. 108–115.
- Woo, S., Abramowitch, S., Kilger, R. and Liang, R., 2006a. "Biomechanics of knee ligaments: injury, healing, and repair". *Journal of biomechanics*, Vol. 39, No. 1, pp. 1–20.
- Woo, S., Fox, R., Sakane, M., Livesay, G., Rudy, T. and Fu, F., 1998. "Biomechanics of the acl: Measurements of in situ force in the acl and knee kinematics". *The Knee*, Vol. 5, No. 4, pp. 267–288.
- Woo, S., Thomas, M. and Saw, S., 2004. "Contribution of biomechanics, orthopaedics and rehabilitation: The past, present and future". *The Surgeon*, Vol. 2, No. 3, pp. 125–136.
- Woo, S., Wu, C., Dede, O., Vercillo, F. and Noorani, S., 2006b. "Biomechanics and anterior cruciate ligament reconstruction". *Journal of Orthopaedic Surgery and Research*, Vol. 1, No. 1, pp. 1–9.

8. RESPONSIBILITY NOTICE

The author Daniel Alejandro Ponce Saldias is the only responsible for the printed material included in this paper.